Polímeros: Ciência e Tecnologia
ISSN: 0104-1428
abpol@abpol.org.br
Associação Brasileira de Polímeros
Brasil

Holanda Saboya Souza, Diego; Tristão Andrade, Cristina; Lopes Dias, Marcos
Effect of Synthetic Mica on the Thermal Properties of Poly(lactic acid)
Polímeros: Ciência e Tecnologia, vol. 24, 2014, pp. 20-24
Associação Brasileira de Polímeros
São Paulo, Brasil

http://dx.doi.org/10.4322/polimeros.2014.053

# Effect of Synthetic Mica on the Thermal Properties of Poly(lactic acid)

**Diego Holanda Saboya Souza, Cristina Tristão Andrade, Marcos Lopes Dias**
***Instituto de Macromoléculas Professora Eloisa Mano, UFRJ***

**Abstract:** Poly(lactic acid)/Somasif fluoromica nanocomposites were prepared by melt blending and their thermal properties investigated by DSC, TGA and DMA. Three different types of synthetic mica (Somasif ME-100, Somasif MAE and Somasif MPE) were used at different contents (2.5, 5.0 and 7.5 wt %). The melt blending of PLA and these micas is characterized by a considerable reduction in the matrix molecular weight, which decreases when the nanofiller content is increased. For all nanocomposites, the thermal stability increases when mica is added to the polymer, with the Somasif MPE, producing the highest increase of the degradation temperature and highest reduction of $T_g$.

**Keywords:** *Poly(lactic acid), synthetic mica, fluoromica, nanocomposites, thermal properties.*

## Introduction

Currently, aliphatic polyesters such as poly(lactic acid) (PLA) have many applications, due to their biodegradability and/or biocompatibility. They are involved inthe manufacture of medical devices, bone surgery, suturing, chemotherapy, etc. and are largely studied as an alternative solution to the environmental problem of plastic waste accumulation, with a special focus on packaging[1,2]. In order to improve the performance of PLA, many studies have been done involving the addition of organophilic nanoclays to the polymer[3-5]. However, little attention has been given to the use of synthetic mica/fluoromica, which is characterized by its high ion exchange capacity and high aspect ratio[6]. In the literature, we have found few studies using synthetic mica nanocomposites[7-9]. We have investigated the preparation of PLA/synthetic micas nanocomposites by melt blending[10-14]. The main purpose of this work was to study the effect of the type and amount of filler on some important thermal properties of these PLA nanocomposites.

## Experimental

### Materials

Poly(L-lactic acid) (PLLA) Ingeo 2002D from NatureWorks were used to prepare the nanocomposites. Three different synthetic fluoromicas (Somasif ME-100, SomasifMAE and SomasifMPE) were obtained from CO-Op Chemical Co (Japan). Somasif ME-100 is a hydrophilic swellable mica with a cation-exchange capacity (CEC) of 120 meq/100 g. Somasif MAE and Somasif MPE are organomodified fluoromicas containing a di-methyl di-hydrogenated tallow ammonium (2M2HTA) and a methyl-diethyl-polypropylene glycol ammonium (M2EPG) as intercalant, respectively[10], where HT are hydrogenated hydrocarbon linear chains, with typical composition C18: 65%, C16: 30% and C14: 5%[15]. According to the manufacturer, the Somasif mica have the general chemical composition: $(Na)_{2x}(Mg)_{3-x}(Si_4O_{10})(F_yOH_{1-y})_2 \cdot nH_2O$, where $0.15 < x < 0.5$; $0.8 < y < 1.0$.

### Sample preparation

In order to eliminate PLA moisture, the polyester was dried for 4 h at 90 °C in a vacuum oven before processing. The synthetic micas, which are also capable of absorbing moisture, were dried under the same conditions.

PLA/Somasif mica nanocomposites with different clay loadings (2.5, 5.0 and 7.5 wt% mica) were prepared in a Coperion ZSK 18 (Werner & Pfleiderer GmbH & Co. KG, Stuttgart, Germany) co-rotating twin-screw extruder, with L/D ratio of 40, at temperatures in the range of 180-200 °C, and screw speed set at 120 rpm. Neat PLA was also processed under the same conditions for comparison purposes.

### Gel Permeation Chromatography (GPC)

Molecular weights of composite matrix (PLA) as well as non-processed PLA granules were measured by using gel permeation chromatography (GPC). Measurements were carried out using an Agilent chromatograph with a Polymer linear column at 25 °C. Chloroform was used as the solvent and the flow rate was 1.0 mL/min with an injection volume of 20 µm. The molecular weight and polydispersity were calculated from a calibration curve made from polystyrene standards with the results expressed as "polystyrene equivalent" molecular weight.

### Thermogravimetric analyses (TGA)

In order to investigate the thermal stability of the composites, thermogravimetric analyses (TGA) were performed. The analyses were done in a TA Instruments Thermoanalyser Q500 from (New Castle, DE, USA). Measurements were carried out under nitrogen flow from room temperature to 700 °C with a heating rate of 20 °C/min.

***Corresponding author: Marcos Lopes Dias**, Instituto de Macromoléculas Professora Eloisa Mano – IMA, Universidade Federal do Rio de Janeiro – UFRJ, Av. Horácio Macedo, 2030, Bloco J, Prédio do Centro de Tecnologia, CEP 21941-598, Rio de Janeiro, RJ, Brasil, e-mail: mldias@ima.ufrj.br*

### *Differencial Scanning Calorimetry (DSC)*

The glass transition temperature ($T_g$) and the melting temperature ($T_m$), as well as the crystallization behavior of the processed materials were evaluated by DSC analysis. The analyses were performed in a TA Instruments equipment, Q1000 model. The samples were thermally treated as follow: 1) heating from 20 to 180 °C and maintained for 1 min at this temperature; 2) rapid cooling to 20 °C; 3) 2nd heating from 0 to 180 °C; 4) cooling to 0 °C at 10 °C/min, and 5) 3rd heating from 0 to 180 °C. All heating runs were performed with a heating rate of 10 °C/min. $T_g$ was obtained from the second heating and $T_m$ from the third heating.

### *Dynamic Mechanical Analysis (DMA)*

Dynamic mechanical properties (storage modulus *E'* and tan δ) of neat PLA and various PLA/synthetic mica composites were measured with Q800 dynamic mechanical TA equipment. Experiments were carried out in the temperature range -20-120 °C at a frequency of 1 Hz with a heating rate of 3 °C/min using a tensile film clamp in strain mode at 0.01 N controlled force. The glass transition temperature, $T_g$, was defined as the temperature at the tan δ peak. The sample specimen dimensions were around 16.5 x 6.5 x 0.6 mm.

## Results and Discussion

### *Molecular weight of PLA*

Table 1 shows the average molecular weight and polydispersity of PLA before and after melt processing with synthetic micas at different compositions.

As expected, PLA processed in the extruder with the synthetic mica has lower molecular weight than that of PLA granules, indicating a certain level of degradation during processing. The reduction in the molecular weight is proportional to the increase in synthetic mica content. The organomica showed the highest effect on the molecular weight reduction when compared to the sodium mica. The degradation during processing leading to reduction in molecular weight has also led to a highest polydispersity ($M_w/M_n$) of the PLA with organomica. These results suggest that, although the synthetic mica presents a high degree of purity as compared with natural clays like montmorillonite, it slightly increases the degree of chain degradation, probably by some catalytic effect. Both, the synthetic mica and its intercalant have hydroxyl groups in their structure which can attack the ester bonds in the PLA chains, causing alcoholysis. Thus it is reasonable to think that the increase of the mica content in the composites generates also an increase of the number of hydroxyl groups, promoting more chain breaking.

### *Thermal stability*

The thermal stability of the nanocomposites was studied by TGA. Figures 1, 2 and 3 show the derivative weight loss versus temperature for the PLA/ME-100, PLA/MAE and PLA/MPE nanocomposites, respectively.

The TG curves of the nanocomposites show an increase in thermal stability compared to neat PLA. The onset temperature ($T_{onset}$), the maximum decomposition temperature ($T_{peak}$) and the concentration of inorganic material (residue), in this case mica, obtained from the TG curves are shown in Table 2.

Although not very significant, the nanocomposite containing sodium mica ME-100 showed an increase in the thermal stability with increasing concentration of mica compared to neat PLA. The organophilic micas led to nanocomposites with better thermal stability. However, with increasing concentration there was a decrease in the $T_{onset}$ and $T_{peak}$. This decrease in thermal stability was associated to the intercalating agents, which begin

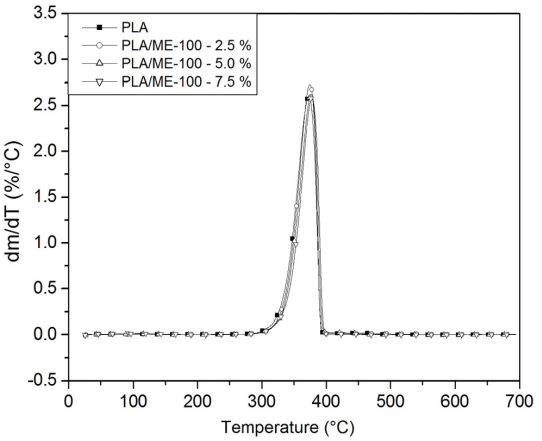


**Figure 1.** DTG curves of PLA and their nanocomposites with Somasif ME-100 synthetic mica.

**Table 1.** Molecular weights and polydispersity of neat PLA and PLA in the PLA/synthetic mica composites.

| Material | Mica (%) | $M_n$ (g/mol) | $M_w$ (g/mol) | $M_z$ (g/mol) | D ($M_w/M_n$) |
|---|---|---|---|---|---|
| PLA | 0 | 121100 | 197000 | 289400 | 1.63 |
| PLA/ME-100 | 2.5 | 81100 | 144100 | 214000 | 1.78 |
| | 5.0 | 85000 | 137700 | 206200 | 1.62 |
| | 7.5 | 84000 | 137400 | 209000 | 1.64 |
| PLA/MAE | 2.5 | 53500 | 112900 | 183500 | 2.11 |
| | 5.0 | 47900 | 106000 | 173500 | 2.21 |
| | 7.5 | 59400 | 102300 | 159500 | 1.72 |
| PLA/MPE | 2.5 | 52300 | 112700 | 180000 | 2.15 |
| | 5.0 | 34200 | 91000 | 159800 | 2.65 |
| | 7.5 | 42000 | 94000 | 151600 | 2.24 |

to degrade before the PLA[10,16]. Therefore, the increase in the intercalant content with increasing concentration of mica leads to a decrease in thermal stability of the nanocomposites. The real concentration values of mica were very close and, in the majority of the cases, slightly superior to those theoretically calculated by carrying out the mixtures.

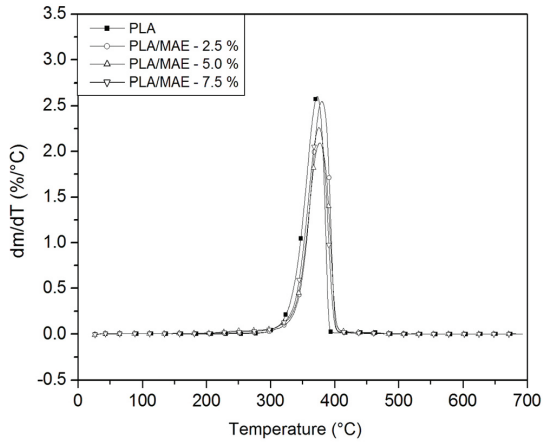


**Figure 2.** DTG curves of PLA and their nanocomposites with Somasif MAE synthetic mica.

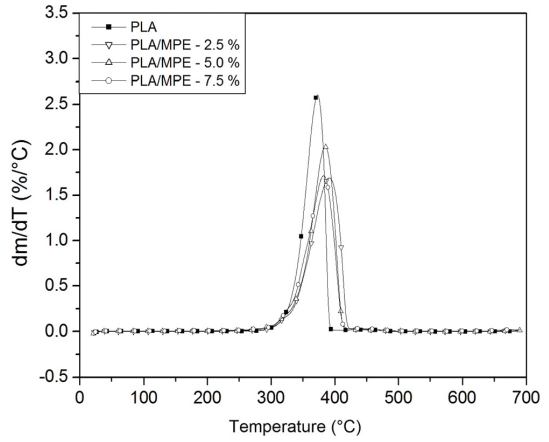


**Figure 3.** DTG curves of PLA and their nanocomposites with Somasif MPE synthetic mica.

**Table 2.** Onset temperature ($T_{onset}$), maximum decomposition temperature ($T_{peak}$) and mica content (residue) of PLA and their nanocomposites with Somasif ME-100, MAE and MPE.

| Material | Degradation temperature (°C) | | Mica content (%) | |
|---|---|---|---|---|
| | $T_{onset}$ | $T_{peak}$ | Theoretical | Experimental |
| PLA | 350 | 373 | 0 | 0 |
| PLA/ME-100 | 351 | 375 | 2.5 | 3.1 |
| | 352 | 376 | 5.0 | 5.7 |
| | 354 | 378 | 7.5 | 7.8 |
| PLA/MAE | 357 | 380 | 2.5 | 2.7 |
| | 351 | 377 | 5.0 | 5.6 |
| | 350 | 376 | 7.5 | 7.5 |
| PLA/MPE | 357 | 391 | 2.5 | 2.5 |
| | 355 | 385 | 5.0 | 4.7 |
| | 349 | 383 | 7.5 | 7.6 |

The higher increase in thermal stability was observed for the nanocomposites containing the MPE mica. This may be due to a better affinity of PLA with the intercalating agent of this mica, which in this case is a quaternary ammonium salt containing a polyether chain, differently from the MAE mica that contains only more apolar alkyl groups. This more polar structure of MPE seems to lead to a better dispersion of this mica in the PLA matrix[10].

### *PLA and nanocomposite thermal transitions*

Table 3 presents data on some thermal properties obtained by DSC. No significant change in the $T_g$ was noted when the synthetic micas are added to PLA, except for Somasif MPE, in which addition of the mica caused a marked decrease in the $T_g$. In this case, as the amount of mica is increased, the $T_g$ decreased reaching 33.7 °C when the concentration was 7.5 wt%. Both, PLA and the nanocomposites presented bimodal melting peaks on heating ($T_{m1}$ and $T_{m2}$) and addition of mica to PLA promoted a decrease in melting temperatures.The major decrease was observed when Somasif MPE was used as the filler for PLA. All the composites did not crystallize during a cooling at 10 °C/min, except the nanocomposites containing the Somasif MPE mica. These differences in the behavior of the Somasif MPE-based nanocomposites and the other PLA/Somasif nanocomposites can be attributed to the high content of intercalant in this commercial synthetic mica[10]. The intercalant seems to be responsible for decreasing the $T_g$ by a plasticizing effect and to promote the speed up of crystallization.

### *Composites dynamic mechanical properties*

Figures 4, 5 and 6 show the dependence of tan δ with temperature for the PLA and their nanocomposites with Somasif micas. Table 4 shows the $T_g$ obtained from the peak of tan δ curves. Note that the addition of mica ME-100 resulted in a small increase in the $T_g$, probably due to a restricted mobility of the chains caused by mica layers. The addition of mica MAE had no significant effect on the $T_g$. However, the addition and increase in mica MPE content led to a decrease in the $T_g$, which is related to the previous mentioned plasticizing effect of the intercalant present in this mica. This is also confirmed by the broadening of the tan δ curves in Figure 6 with the increase in mica content.

Figures 4, 5 and 6 also show that the addition of mica led to a decrease in the intensity of tan δ curves. Since tan δ is a measure of the relative energy distribution in the sample, i.e. it is the ratio between the dissipated energy and the elastic energy of the system, this decrease in tan δ is due to the more pronounced increase of the storage modulus as compared to the loss modulus, which is related to a lower dissipation of mechanical energy in the sample. The addition of mica helped to distribute and store the energy during deformation. This is reflected by a decrease in tan δ as the mica content increases[17]. The decrease in tan δ intensity is more pronounced for the

**Table 3.** Crystallinity and thermal transitions of PLA and PLA/synthetic mica nanocomposites.

| Sample | Mica (%) | $T_g$ (°C) | $T_{m1}$ (°C) | $T_{m2}$ (°C) | $\Delta H_m$ (J/g) | $T_{ch}$ (°C) | $\Delta H_{ch}$ (J/g) | $T_{cc}$ (°C) | $\Delta H_{cc}$ (J/g) |
|---|---|---|---|---|---|---|---|---|---|
| PLA | | 59.9 | 153.3 | - | 17.5 | 131.2 | 16.9 | - | - |
| | 2.5 | 59.6 | 152.1 | - | 26.5 | 128.5 | 23.2 | - | - |
| PLA/ME-100 | 5.0 | 59.6 | 151.9 | - | 27.9 | 126.2 | 25.6 | - | - |
| | 7.5 | 60.2 | 153.0 | 157.4 | 31.1 | 124.2 | 28.7 | - | - |
| | 2.5 | 60.6 | 149.0 | 157.5 | 32.0 | 109.2 | 34.1 | - | - |
| PLA/MAE | 5.0 | 59.9 | 147.6 | 156.4 | 32.6 | 105.9 | 30.8 | - | - |
| | 7.5 | 58.4 | 146.6 | 155.6 | 32.8 | 103.6 | 29.1 | - | - |
| | 2.5 | 53.5 | 144.8 | 154.8 | 33.1 | 96.5 | 29.0 | 91.7 | 3.6 |
| PLA/MPE | 5.0 | 40.6 | 138.0 | 149.8 | 33.9 | 131.2 | 16.9 | 90.1 | 28.5 |
| | 7.5 | 33.7 | 132.6 | 146.4 | 29.9 | 128.5 | 23.2 | 91.9 | 26.2 |

$T_{m1}$ and $T_{m2} = T_m$ of bimodal melting peak; $T_{cc}$ = crystallization temperature during cooling; $T_{ch}$ = crystallization temperature during heating; $\Delta H_m$, $\Delta H_{ch}$ and $\Delta H_{cc}$ = enthalpies of melting, crystallization during heating and crystallization during cooling, respectively.

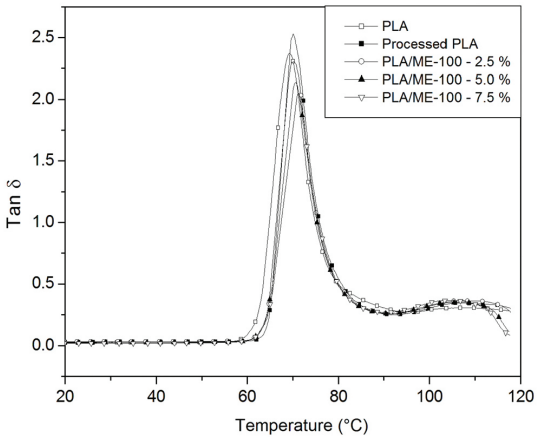


**Figure 4.** Dependence of temperature on tan δ for neat non-processed PLA, processed PLA and PLA/Somasif ME-100 nanocomposites.

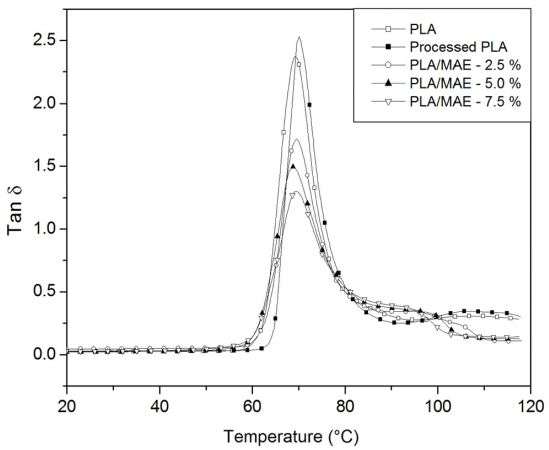


**Figure 5.** Dependence of temperature on tan δ for neat non-processed PLA, processed PLA and PLA/Somasif MAE nanocomposites.

composites with the MPE mica that could be explained by the better dispersion of this mica in the polymer matrix and by the higher amount of intercalant present in this mica[14].

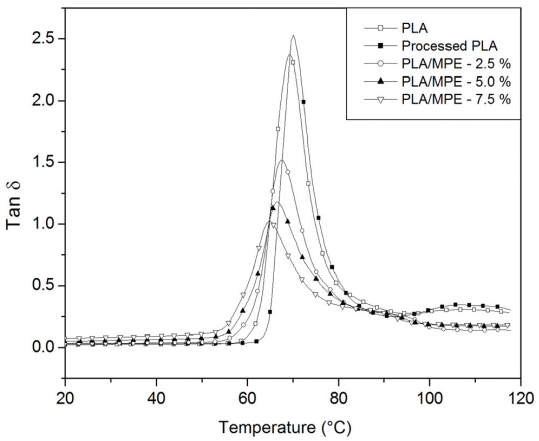


**Figure 6.** Dependence of temperature on tan δ for neat non-processed PLA, processed PLA and PLA/Somasif MPE nanocomposites.

**Table 4.** $T_g$ of PLA and PLA/Somasif composites obtained from tan δ.

| Material | Mica content (%) | $T_g$ (°C) |
|---|---|---|
| PLA | 0 | 69.3 |
| Processed PLA | 0 | 70.1 |
| | 2.5 | 70.2 |
| PLA/ME-100 | 5.0 | 70.6 |
| | 7.5 | 71.2 |
| | 2.5 | 69.4 |
| PLA/MAE | 5.0 | 68.8 |
| | 7.5 | 69.5 |
| | 2.5 | 67.4 |
| PLA/MPE | 5.0 | 66.6 |
| | 7.5 | 65.1 |

## Conclusions

Somasif synthetic micas which are non-expensive nanofillers can be used to produce PLA nanocomposites by melt processing with possible application in packaging. The melt processing of PLA and these micas is characterized by a considerable reduction in the molecular weight, which decreases with the increase

of nanofiller content. All micas increased the thermal stability of the composites, but the Somasif MPE which contains a polyether-based ammonium salt produced the highest increase in degradation temperature ($T_{max}$). This mica also led to the most significant decrease in the $T_g$ of PLA/Somasif nanocomposites and increase of the crystallization rate of PLA.

## Acknowledgments

The authors are grateful to CNPq, CAPES and FAPERJ for the financial support and to Professor Chiaki Azuma of the Open University of Japan, Japan, for donating the Somasif micas.

## References

1. Hyon, S. H.; Jamshidi, K. & Ikada, Y. - Biomaterials, **18**, p.1503 (1997). http://dx.doi.org/10.1016/S0142-9612(97)00076-8
2. Paul, M. A.; Alexandre, M.; Degee, P.; Henrist, C.; Rulmont, A. & Dubois, P. - Polymer, **44**, p.443 (2003). http://dx.doi.org/10.1016/S0032-3861(02)00778-4
3. Di, Y.; Iannace, S.; Maio, E. D. & Nicolais, L. - J. Polym. Sci., Part B: Polym. Phys., **43**, p.689 (2005). http://dx.doi.org/10.1002/polb.20366
4. Pluta, M.; Galeski, A.; Alexandre, M.; Paul, M. A. & Dubois, P. - J. Appl. Polym. Sci., **86**, p.1497 (2002). http://dx.doi.org/10.1002/app.11309
5. Ray, S. S.; Yamada, K.; Okamoto, M. & Ueda, K. - Polymer, **44**, p.857 (2003).
6. Carrado, K. A.; Csencsits, R.; Thiyagarajan, P.; Seifert, S.; Macha, S. M. & Harwood, J. S. - J. Mat. Chem.,**12**, p.3228 (2002). http://dx.doi.org/10.1039/b204180b
7. Ray, S. S. & Okamoto, M. - Macromol. Rapid Commun., **24**, p.815 (2003). http://dx.doi.org/10.1002/marc.200300008
8. Chu, L. L.; Anderson, S. K.; Harris, J. D.; Beach, M. W. & Morgan, A. B. - Polymer., **45**, p.4051 (2004). http://dx.doi.org/10.1016/j.polymer.2004.03.012
9. Hsieh, T. H.; Huang, J. K.; Ho, K. S.; Bi, X.; Ho, T. H.; Yang, S. S. & Chang, Y. C. - J. Polym. Sci. Part B: Polym. Phys. **46**, p.1214 (2008). http://dx.doi.org/10.1002/polb.21455
10. Souza, D. H. S.; Dahmouche, K.; Andrade, C. T. & Dias, M. L. - Appl. Clay Sci., **54**, p. 226 (2011). http://dx.doi.org/10.1016/j.clay.2011.09.006
11. Souza, D. H. S.; Borges, S. V.; Dias, M. L. & Andrade, C. T. - Polym. Compos., **33**, p.555 (2012). http://dx.doi.org/10.1002/pc.22177
12. Borges, S. V.; Dias, M. L.; Pita, V. J. R. R.; Azuma, C. V. & Dias, M. V. - J. Plast. Film Sheet., **28**, p.1-15 (2012).
13. Souza, D. H. S.; Dias, M. L.; Andrade, C. T. - Mat. Sci. Eng. C, **33**, p.1795 (2013). PMid:23827638. http://dx.doi.org/10.1016/j.msec.2012.12.091
14. Souza, D. H. S.; Dahmouche, K.; Dias, M. L. & Andrade, C. T. - Appl. Clay Sci., **80-81**, p.259 (2013). http://dx.doi.org/10.1016/j.clay.2013.04.012
15. Bordes, P.; Pollet, E. & Avérous, L. - Prog. Polym. Sci., **34**, p.125 (2009). http://dx.doi.org/10.1016/j.progpolymsci.2008.10.002
16. Barbosa, R.; Araújo, E. M.; Melo, T. J. A. & Ito, E. N. - Polímeros, **17**, p.104 (2007).
17. Camponeschi, E. L. - "Dispersion And Alignment Of Carbon Nanotubes In Polymer Based Composites", PhD Thesis, Georgia Institute of Technology, United States (2007).

*Received: 01/31/13*
*Revised: 05/28/13*
*Accepted: 10/02/13*